International Journal of GEOMATE, July, 2025 Vol.29, Issue 131, pp.95-103
ISSN: 2186-2982 (P), 2186-2990 (O), Japan, DOI: https://doi.org/10.21660/2025.131.4985
Geotechnique, Construction Materials and Environment

EXPERIMENTAL STUDY OF FACTORS AFFECTING ULTRASONIC PULSE TIME IN FIBER-REINFORCED CONCRETE

Thi Nhan Pham[1], Huy Viet Le[1] , Van Duc Bui[1], Van Manh Nguyen[1] and *Van Phi Dang[1]

[1]Faculty of Civil Engineering, Hanoi University of Mining and Geology, Hanoi, Vietnam

*Corresponding Author, Received: 02 April 2025, Revised: 27 April 2025, Accepted: 28 April 2025

ABSTRACT: This study investigates factors affecting ultrasonic pulse propagation time (UPPT) in high-performance fiber-reinforced concrete (HPFRC). Steel fiber contents (0.0, 0.5, 1.0, and 2.0 vol%), specimen sizes (40×40×160 mm³ and 150×150×600 mm³), the presence of cracks, and different measurement methods on UPPT in HPFRC, were considered. Bending and compression tests were used to determine both the UPPT and mechanical properties of matrices. Steel fibers significantly affect the UPPT of HPFRC, especially under post-loading conditions, by improving crack bridging and preserving structural integrity, thus delaying pulse attenuation. HPFRC without steel fibers fails to transmit pulses after loading as a result of severe cracking, whereas HPFRC with 0.5%, 1.0%, and 2.0% steel fibers increases pulse propagation time, with higher fiber content providing better resistance to crack propagation. Besides, larger specimens exhibit longer UPPT due to energy attenuation, wave interaction, and material heterogeneity, but this effect diminishes as fiber content exceeds 1.0%. Furthermore, the direct measurement method consistently produces lower UPPT than the indirect measurement method due to shorter pulse travel distances. In addition, vertical notches also impact UPPT, with longer propagation times as cracks widen. Under increasing bending stress, UPPT becomes unstable, and excessive crack expansion disrupts signal transmission.

Keywords: Ultrasonic pulse propagation time, High-performance fiber-reinforced concrete, Non-destructive testing method, Steel fiber content, Size effect

1. INTRODUCTION

High-performance fiber-reinforced concrete (HPFRC) has gained widely use in civil engineering due to its superior mechanical properties, such as enhanced strength and durability [1,2]. Fibers are incorporated into HPFRC to enhance its tensile strength, ductility, and durability by bridging cracks, fostering strain-hardening, and mitigating shrinkage cracking in the hardened concrete [3]. However, the complex microstructure of HPFRC arises from several factors, including its dense cementitious matrix with a high binder content and low water-to-cement ratio, the multi-scale composition of materials such as fine aggregates, cementitious binders, and fibers that create a hierarchical structure, and the presence of interfacial transition zones (ITZ) between fibers, aggregates, and the matrix, which are often weaker and more heterogeneous than the bulk material [4]. Thus, there are significant challenges in the process of evaluating the structural durability of HPFRC, especially in terms of identifying internal defects and monitoring its degradation over time [1,3].

Non-destructive testing methods (NDTMs) have gained considerable traction in recent years, presenting a more economical and feasible option for evaluating the strength of materials [4,5]. A non-destructive evaluation technique based on the measurement of ultrasonic pulse velocity (UPV) in concrete is widely applied to determine the mechanical properties and internal structure of concrete [6,7,18]. This method provides insights into the homogeneity, strength, and potential defects of concrete, making it a valuable non-destructive testing method for assessing concrete integrity and performance. The findings of previous studies have demonstrated the strong potential of NDTMs in estimating concrete strength. However, the reliability of this method depends on the accurate determination of the ultrasonic pulse propagation time (UPPT) [8].

Numerous studies have investigated the propagation of ultrasonic pulses in conventional and fiber-reinforced concretes, focusing on parameters such as material composition, curing conditions, and fiber content. AL-Ridha et al. [9] examined the UPV in self-compacting concrete (SCC) using two volume fractions of steel fibers (0.4% and 0.8%) in 100 mm cubes and 200 mm cylinders. The UPV of SCC increased with higher steel fiber content, with a greater percentage increase in cylinders compared to cubes. For the same steel fiber fraction, the UPV of SCC decreases as specimen length increases, from 100 mm cubes to 200 mm cylinders. The effects of specimen length on UPV diminish as steel fiber content increases [9]. In [10], researchers examined the influence of varying steel reinforcement ratios (0.8%, 1.0%, 1.2%, and 1.4%) on the prediction of UPV in concrete beams. Their findings revealed that the UPV increased proportionally with the percentage of reinforcement in the beams. Petro J. T. and Kim J [11] evaluated the delamination in slabs with thicknesses of 150 mm and 300 mm by employing the

UPV method. A qualitative correlation was identified between the P-wave transit time and delamination size. Moreover, wave diffraction at the delamination edges contributed to a reduction in wave velocity. Ersoy et al. [11] investigated the relationship between sample length and diameter and compressional wave velocity. They reported that in the direct measurement method, the ultrasonic wave velocity remains unaffected by the sample size and diameter. The differing results were attributed to factors such as weathering, micro-fissure ratio, and heterogeneity rather than to sample sizes. Pahlavan et al. [12] investigated the interaction of ultrasonic waves with partially closed surface cracks in concrete structures. They considered the effects of crack width, wave incidence angle, and distance from the cracks on travel time and wave amplitude as concrete beams were unloaded. The travel time was largely unaffected by the crack opening (0.05 mm to 3 mm). Significant anisotropy was observed in both orthogonal and parallel directions to the crack within the cracked zone. Malhotra and Carino [12] summarized a comprehensive review of non-destructive methods for evaluating conventional concrete. However, the inclusion of notched specimens and the application of dual measurement techniques were specifically designed to overcome limitations in previous studies, in which the effects of crack propagation and the differences between measurement methods on UPPT have not been fully explored. Although previous research has examined the effects of steel fibers and steel bar content on the UPV of concrete, the influence of other factors, such as curing conditions, fiber type, and environmental exposure, remains underexplored, particularly for HPFRC. Moreover, there is a significant gap in the available literature regarding the influence of specimen size and shape on UPV, highlighting the need for further comprehensive research in HPFRC.

This study investigated the key parameters influencing the propagation time of ultrasonic pulses in HPFRC. The findings are expected to enhance non-destructive testing methods, providing a reliable and efficient approach for evaluating the quality and performance of HPFRC in practical applications. The primary goals of this study were to analyze (1) the influence of steel fiber contents, (2) the effect of specimen sizes, (3) the role of notches in specimens, and (4) the effect of various measurement methods in the UPPT of HPFRC.

2. RESEARCH SIGNIFICANCE

This study investigates the UPPT in HPFRC, considering the effects of steel fiber content, specimen size, pre-formed cracks, flexural-induced cracks, and different measurement techniques. In addition, it explores real-time variations of UPPT under bending stress during flexural testing. Although previous studies have primarily examined these parameters individually or focused on conventional concrete, the present research provides new insights into their combined effects on HPFRC. The findings are expected to support the optimization of fiber dosage, specimen design, and testing methods. Moreover, they aim to enhance the reliability of HPFRC applications and advance the development of more effective non-destructive evaluation techniques for structural health monitoring and assessment.

3. MATERIALS AND METHODS

Table 1 provides a summary of the HPFRCC compositions based on the weight ratio of cement, as referenced in [13]. Experimental tests were conducted to investigate the influence of varying fiber content levels on the pulse propagation time of HPFRCC under bending conditions. The abbreviations SF00, SF05, SF10, and SF20 refer to the steel fiber volume contents in the specimens of matrices, with values of 0.0 vol%, 0.5 vol%, 1.0 vol%, and 2.0 vol%, respectively (Table 1). Steel fibers have a diameter of 0.2 mm, a length of 13 mm, and an elastic modulus of 200 GPa. In order to explore the effect of cracks on ultrasonic pulse propagation, a single vertical notch was pre-created in the experimental specimens. The notations N0 and N1 refer to the number of notches in the specimen of the matrices.

Table 1. Matrix component ratios by cement weight

Cement	Silica fume	River sand	W/C	SP
1.0	0.25	1.25	0.2	0.035

A 30-liter mixer was utilized to achieve thorough and uniform mixing of the materials. The initial mixing process involved the dry ingredients, including silica fume and cement, for approximately 3 minutes. River sand was subsequently added and mixed for 5 minutes. Next, water was added gradually and mixed for 2 minutes to achieve uniformity. A superplasticizer was then incorporated and mixed for another 2 minutes. Flow values, measured using a mini cone on fresh mixtures, were controlled within the range of 240 to 260 mm to ensure the uniform dispersion of fibers. Finally, steel fibers were manually added and mixed for 2 minutes.

Bending tests were conducted on two specimen sizes (40×40×160 mm³ and 150×150×600 mm³) using three-point bending in three dimensions. The dimensions of the compressed specimens are 50×50×50 mm³. All specimens were covered with a plastic sheet to maintain the laboratory temperature at 25 ± 2 °C, controlling relative humidity within the 50–70% range during UPV testing to reduce variability and enhance the accuracy of measurements. After 48 hours, they were removed

from the molds and transferred to a hot water tank kept at 80 ± 5 °C for 72 hours.

An ADVANTEST 9 machine with a 3000 kN capacity was used to perform the three-point bending test, as shown in Fig. 1. The loading rates are 0.05 MPa/s for 150×150×600 mm³ and 0.1 MPa/s for 40×40×160 mm³ specimens. Besides, compressive tests were conducted on the ADVANTEST 9 testing machine at a loading rate of 0.5 MPa/s. In addition, the UPPT of the matrices was determined using the PULSONIC 58-E4900 ultrasonic pulse analyzer, which complies with EN 12504-4 and ASTM C597 standards. The primary focus of these standards lies in the testing methodology, the accurate interpretation of UPV measurements, and the provision of detailed procedures for conducting UPV testing. This device features a highly precise transit time measurement function, with a nominal frequency of 50 kHz and a generator pulse voltage of 2500 V. Moreover, the position of the transducers was carefully marked with precise dimensions to ensure the accuracy of repeated measurements at the same location.

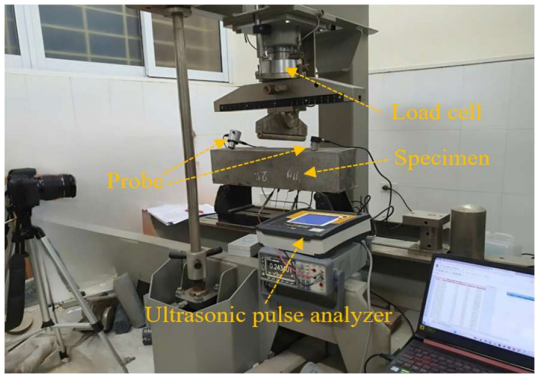

Fig. 1 A test set up for measuring the UPPT and flexural strength of specimens under bending tests

4. RESULTS AND DISCUSSION

4.1 Mechanical Properties of HPFRC

The compressive strength of matrices exhibits a slight increase as the steel fiber content rises from 0.0% to 1.0%, but subsequently declines when the fiber content reaches 2.0%. The compressive strength of SF00N0, SF05N0, and SF10N0 was 63.95, 92.88, and 101.31 MPa, respectively, whereas that of SF20N0 was 86.06 MPa. The decline in compressive strength of matrices observed at 2.0% fiber content may result from poor workability and fiber agglomeration, which lead to non-uniform fiber distribution and increased porosity in the matrix [14].

In addition, fiber contents significantly influenced the flexural strength of the matrices. Specifically, the incorporation of 0.5%, 1.0%, and 2.0% steel fibers enhanced the flexural strength of matrices with specimen sizes of 150×150×600 mm³ by 28.68%, 30.75%, and 51.42%, respectively. Similarly, incorporating 0.5% and 2.0% steel fibers increased the flexural strength of 40×40×160 mm³ specimens by 58.04% and 60.91%, respectively. The increase in flexural strength with higher steel fiber contents can be attributed to the enhanced bridging effect provided by the fibers (Fig. 2), which improves the resistance to micro-cracking and the redistribution of stresses within the matrix. Besides, the observed variation in flexural strength enhancement across different specimen sizes indicates the influence of size effects, with smaller specimens (40×40×160 mm³) exhibiting a more pronounced percentage increase compared to larger ones (150×150×600 mm³).

Furthermore, the reduction in flexural strength of SF10N1 (8.24 MPa) compared to SF10N0 (10.12 MPa), despite having the same fiber content (1.0%), highlights the influence of structural discontinuities on mechanical performance. The presence of a pre-formed vertical notch in SF10N1 effectively reduces the effective cross-sectional height, leading to a diminished load-bearing capacity. This aligns with fracture mechanics principles, where stress concentrations around notches initiate and propagate cracks more readily, accelerating failure [15].

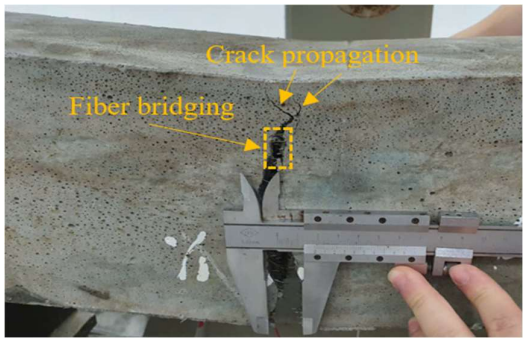

Fig. 2 Effect of steel fiber on crack propagation

4.2. Effect of Steel Fiber Contents on UPPT Behavior in HPFRC

Table 2 provides the UPPT in matrices under conditions before and after loading. The increase in steel fiber content generally enhances its ability to transmit ultrasonic pulses, especially under post-loading conditions. Initially, the matrices without any notches (SF00N0) exhibit relatively higher UPPT values, particularly for the IMM, with a value of 244.6 μs under pre-loading and a complete absence of pulse propagation post-loading (0.0 μs). In contrast, matrices incorporating steel fibers (SF05, SF10, SF20) demonstrate varying responses, with post-loading IMM values revealing a significant increase in UPPT. Furthermore, the presence of vertical notches in the specimens had a significant effect on UPPT values. For example, the SF10N1 specimen,

which contains both a fiber content (1.0 vol%) and a notch (N1), experienced a substantial increase in UPPT, rising from 208.4 μs (pre-loading) to 530.4 μs (post-loading) for the DMM, and from 244.4 μs to 687.0 μs for the IMM.

In addition, a comparison of the two measurement methods (DMM and IMM) reveals that IMM consistently produces higher UPPT values, especially in post-loading conditions. For instance, in the SF05N0 specimen, the UPPT increased from 203.5 μs (pre-loading) to 521.5 μs (post-loading) using IMM, while the DMM values rose from 140.3 μs to 205.0 μs. Similarly, in SF10N0, IMM recorded an increase from 208.4 μs to 530.4 μs, whereas DMM values escalated from 141.0 μs to 419.1 μs. The difference is even more pronounced in SF10N1, where IMM values rose from 244.4 μs to 687.0 μs, while DMM values increased from 166.8 μs to 427.9 μs. These findings suggest that IMM is more responsive to material heterogeneity, crack propagation, and the presence of notches in matrices. In contrast, DMM values remain lower, possibly due to its localized measurement method, which may not entirely reflect crack-induced disturbances in the propagation path.

Table 2. UPPT of matrices under pre-loading and post-loading conditions

Matrix	Pre-loading condition		Post-loading condition	
	DMM (μs)	IMM (μs)	DMM (μs)	IMM (μs)
SF00N0	158.1	244.6	0.0	0.0
SF05N0	140.3	203.5	205.0	521.5
SF10N0	141.0	208.4	419.1	530.4
SF20N0	145.0	171.9	316.4	417.1
SF10N1	166.8	244.4	427.9	687.0

4.3. Influence of Specimen Dimensions on UPPT in HPFRC

Matrices with larger sample sizes exhibited longer UPPT than those with smaller samples. For instance, the UPPT of the same SF00N0 matrix was 73.9 μs for a size of 150×150×600 mm³ and 49.1 μs for 40×40×160 mm³, as shown in Fig. 3. The increased UPPT in the larger specimens, as compared to the smaller ones, can be attributed to factors like energy attenuation, wave interaction, and material heterogeneity [16].

Additionally, HPFRC containing steel fibers exhibited a lower UPPT than HPFRC without steel fibers. As an example, for a specimen size of 150×150×600 mm³, the UPPT of the SF00N0 matrix, which did not contain any steel fiber contents, was 73.9 μs. In contrast, the UPPTs of matrices with 0.5 vol%, 1.0 vol%, and 2.0 vol% steel fiber contents (SF05N0, SF10N0, SF20N0) were 71.6 μs, 57.3 μs, and 60.1 μs, respectively (Fig. 3). This behavior can be attributed to changes in the microstructure of the concrete mix upon the addition of steel fibers. Firstly, the incorporation of steel fibers enhances ultrasonic wave transmission within the material. The presence of steel fibers in the concrete matrix reduces porosity and increases material homogeneity, allowing ultrasonic waves to propagate more efficiently [17]. However, as the steel fiber content surpassed 1.0%, the influence of sample size on UPPT became nearly insignificant, although the UPPT experienced a slight increase at a steel fiber content of 2.0% (SF20N0) compared to 1.0% (SF10N0). This occurrence could be attributed to fiber clustering at higher dosages, potentially increasing local porosity and impairing ultrasonic wave propagation, as in [8]. Achieving uniform fiber dispersion remains a significant challenge, particularly at high fiber volumes, where agglomeration may reduce the overall homogeneity of specimens. Consequently, limitations such as the difficulty in maintaining uniform fiber dispersion at high fiber contents should be carefully evaluated. Furthermore, the UPV method has its limitations, including sensitivity to surface imperfections and difficulty in detecting small or deeply embedded defects in specimens.

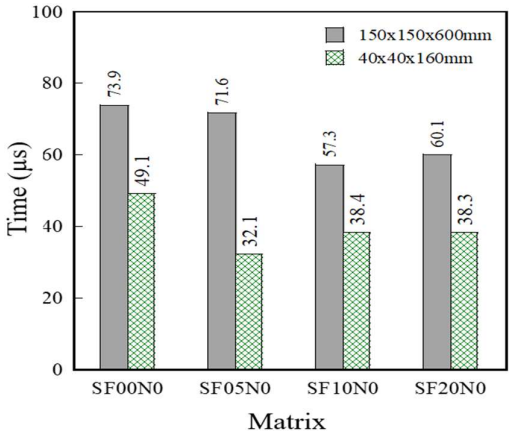

Fig. 3 Size effect on ultrasonic pulse propagation time in matrices

4.4. Influence of Measurement Technique on UPPT in HPFRC

The UPPT values in all matrices at both before and after loading conditions when using the DMM were smaller than those using the IMM. For instance, the UPPT values of SF05N0 using DMM and IMM techniques at the pre-loading condition were 140.3 μs and 203.5 μs, respectively, while at the post-loading condition, they were 205 μs and 521.5 μs, respectively (Figs. 4a-b). However, in the control matrix (SF00N0), the specimens fail abruptly under bending stress, preventing the measurement of pulse

propagation time once the maximum bending stress is reached (Fig. 4b).

The fiber content has a significant influence on the UPPT of the matrices, especially in the post-loading state. After loading, the UPPT discrepancies of matrices between techniques DMM and IMM corresponding to fiber contents of 0.5%, 1.0%, and 2.0% were 154.4%, 26.56%, and 31.82%, respectively. Besides, the UPPT differences of matrices with a vertical notch and 1.0% fiber content (SF10N1) remained relatively stable both before and after loading as the techniques DMM and IMM were applied. The UPPT variations of SF10N1 both before and after loading as the techniques DMM and IMM were applied, with values of 46.52% and 60.55%, respectively. The difference in UPPT values between the DMM and IMM techniques has also been reported in the literature [19], with variations ranging from 5% to 20%, primarily influenced by the quality of concrete. This difference may result from wave dispersion during propagation through the concrete structure [20].

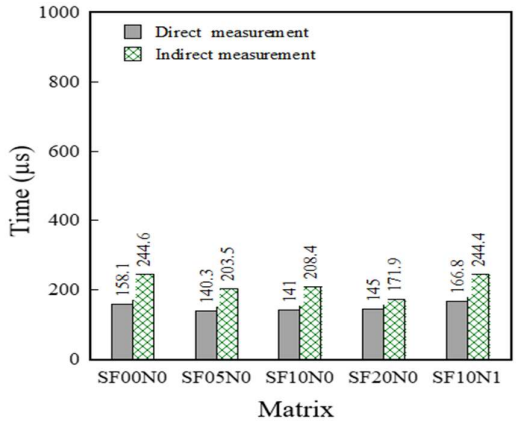

a) Before loading condition

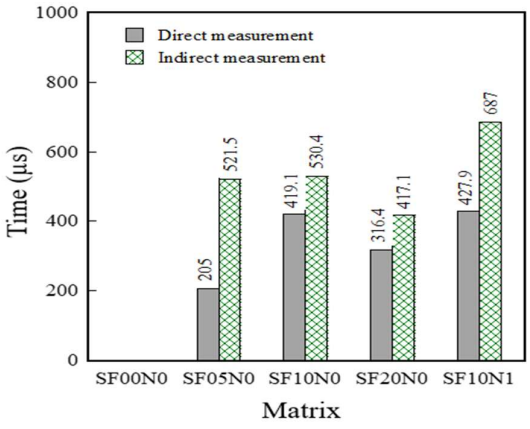

b) After loading condition

Fig.4 Comparison of the UPPT in matrices before and after loading conditions

In the DMM technique, the ultrasonic pulse propagates along a straight-line path directly between the transmitter and the receiver, thereby minimizing the travel distance and resulting in a shorter propagation time. Conversely, in the IMM technique, the ultrasonic pulse travels at an angle, frequently reflecting off boundaries or interfaces, such as the edges of the sample, before reaching the receiver. This extended travel path increases the effective propagation distance and subsequently lengthens the propagation time [21]. Besides, in terms of energy dissipation, the indirect method involves a longer path and additional reflections compared to the direct method, resulting in greater energy loss through scattering and absorption in the concrete. This causes a slight reduction in wave velocity, increasing the time needed to reach the receiver [22]. Furthermore, HPFRCC is a heterogeneous and highly porous material, as a result, the ultrasonic pulse of the IMM follows a longer and more complex path, leading to slower wave propagation compared to the DMM [21]. The application of simulation-based techniques would support the validation of the proposed mechanisms underlying energy dissipation and wave reflection in relation to higher IMM values. Future studies should consider advanced numerical modeling, such as finite element analysis, to explore these effects in deeper understanding.

4.5. Influence of Cracks on UPPT in HPFRC

The UPPT values of matrices containing 1.0% steel fiber content, with specimens having a vertical notch and those having no vertical notch, were measured under both pre-loading and post-loading conditions (Table 2). The vertical notches had a significant effect on the UPPT values in both DDM and IMM techniques. Under pre-loading conditions, the SF10N1 matrix exhibited a 17.3% increase in UPPT with the IMM method and an 18.3% increase with the DMM method, relative to the control matrix (SF10N0). In contrast, under post-loading conditions, the UPPT of SF10N1 increased by 2.1% with the DMM technique, and by 30% with the IMM technique, compared to the matrix control (SF10N0). This can be explained by the fact that as the crack widens and its depth increases, the wave propagation distance grows, leading to stronger wave reflections. This results in the pulse waves reaching the signal receiver later, increasing the pulse wave propagation time.

Under flexural loading, steel fibers prevent sudden failure in matrices by bridging cracks, causing a noticeable difference in pulse propagation times of matrices between those with and without fiber contents. Matrices without steel fibers undergo complete failure, rendering pulse measurement impossible after destruction. Conversely, matrices containing steel fibers retain measurable pulse

propagation times, even though the pulse propagation time increased markedly compared to before the application of bending loads [23]. The expansion of cracks under bending stress becomes more pronounced as the steel fiber content increases. The crack widths of SF05N0, SF10N0, and SF20N0 were measured at 10 mm, 12 mm, 19 mm, and 23 mm, respectively, as shown in Fig. 5. Furthermore, the crack width of SF10N1 matrix (23 mm), which contains 1.0% steel fiber, is larger than that of SF20N0 (19 mm), which is used 2.0% steel fiber. The presence of cracks in concrete significantly impacts the ultrasonic pulse propagation time, leading to diffraction and an increase in propagation time. This effect can be explained by the shape, width, and orientation of the cracks influencing how the waves are scattered or reflected, altering the signal intensity and propagation time [11].

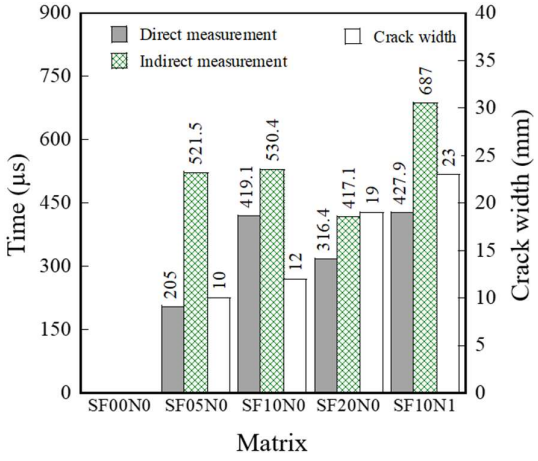

Fig. 5 Relationship between pulse propagation time and crack width after testing

The UPPT for the SF10N0 and SF10N1 specimens was obtained prior to applying flexural loading, using the IMM to evaluate the effect of the notch in the specimens at different measurement distances parallel to the vertical notch. The wave propagation trend in the specimens is generally consistent, with a significant increase in UPPT as the propagation distance increases. With a steel fiber content of 1.0%, the difference in UPPT between specimens with and without notches is as high as 50%, reaching up to 84.6%, as the transducer distance is below 150 mm.

However, as the distance between the transducers exceeds 400 mm, the sensitivity in detecting cracks gradually decreases. Specifically, the difference in UPPT between the notched and unnotched specimens is less than 20%. This indicates that when the transducer distance is around 150 mm, the UPPT is most sensitive to the presence of the notch. This finding is consistent with the guidelines outlined in [24], which highlight the effect of transducer distance on the accuracy of ultrasonic pulse velocity testing. According to the operating instructions, the ideal distance between the transducer and the notch for optimal test accuracy is 150 mm.

4.6. Correlation of Wave Propagation Time with Bending Stress in Concrete

Fig. 6 illustrates the relationship between UPPT values, reflecting pulse propagation time, and the percentage of bending stress in high-strength concrete during flexural tests. During a period of less than 40 s, as the bending stress ratio remains below 37%, specimens maintain their elastic state. Consequently, the UPPT remains stable at a value of 166.7μs and exhibits no significant variation, as shown in Fig. 7a. As the bending stress ratio progresses from 37% to less than 100%, cracks form and widen under bending stress.

In this phase, the UPPT experiences instability and fluctuates with multiple transitions. The corresponding UPPT values during this stage increase from 166.7 μs to 279.8 μs, as shown in Fig. 7b. As the stress exceeds 100%, the cracks undergo excessive expansion, leading to the loss of the pulse signal and signal disruption. This causes the UPPT to suddenly increase to 667.0 μs. This can be attributed to the scattering of pulse energy, which prevents the signal from effectively reaching the receiver, primarily due to the formation and progressive expansion of deeper cracks [25,26,27]. The irregular fluctuations observed in the UPPT signal underscore the nonlinear behavior of the material when subjected to flexural loading. To gain a more comprehensive understanding of this response, future research should consider the application of advanced signal processing techniques, such as wavelet or spectral analysis.

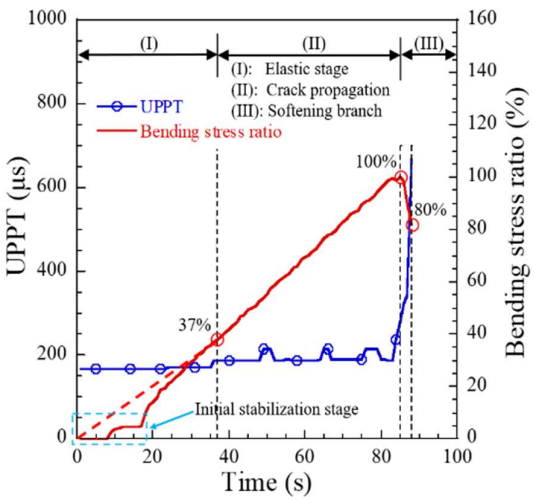

Fig. 6 Dependence of wave propagation time on bending stress in concrete

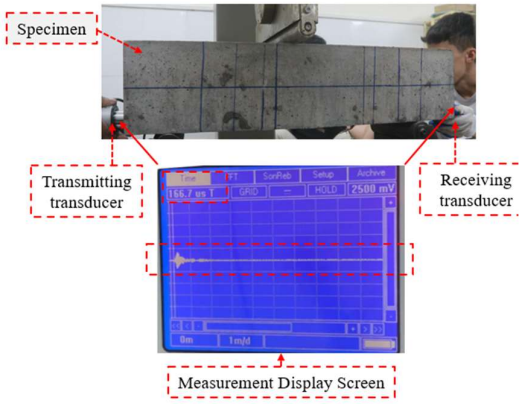

a) Before the first cracking state

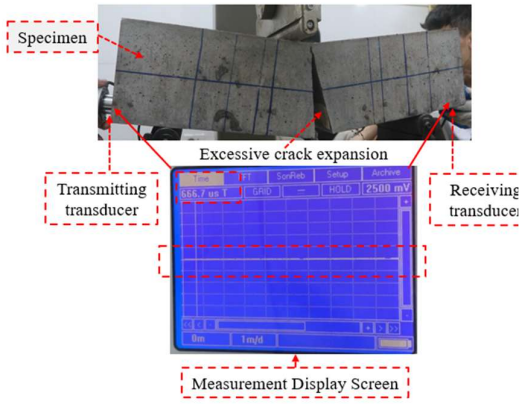

b) After post-cracking state

Fig. 7 Images of pulse signals and crack propagation under bending loads

5. CONCLUSION

This study presents a comprehensive experimental investigation into the factors influencing the UPPT in HPFRC. The results emphasize the significant effects of steel fiber content (0.0 vol%, 0.5 vol%, 1.0 vol%, and 2.0 vol%), specimen sizes (40×40×160 mm³ and 150×150×600 mm³), the presence of cracks, and the influence of different measurement methods on the UPPT of HPFRC. The experimental observations and their related implications are summarized in the following points:

- The incorporation of steel fibers significantly influences UPPT in matrices, particularly under post-loading conditions, by enhancing crack bridging and preserving structural integrity, thereby delaying pulse attenuation under applied loads. The matrix without steel fibers fails to transmit pulses after loading due to severe cracking. In contrast, matrices with 0.5 vol%, 1.0 vol%, and 2.0 vol% steel fibers exhibit an increased pulse propagation time, with higher fiber content offering better resistance to crack propagation.
- The size of the specimen has a significant effect on UPPT in matrices, with larger specimens exhibiting longer UPPT values than smaller ones. Specifically, the UPPT measured for the SF00N0 matrix was 73.9 μs with a specimen size of 150×150×600 mm³, compared to 49.1 μs for a smaller specimen of 40×40×160 mm³. This longer UPPT in larger specimens is associated with factors such as energy attenuation, wave interaction, and material heterogeneity. In addition, matrices containing steel fibers exhibited lower UPPT values compared to those without fibers. Besides, as the steel fiber content exceeds 1.0%, the effect of sample size on UPPT became nearly insignificant.
- The DMM consistently resulted in smaller UPPT values compared to the IMM, due to the shorter travel path of the pulse in the direct method. For example, under before loading conditions, the UPPT values recorded for SF05N0 were 140.3 μs with the DMM method and 203.5 μs with IMM. Besides, fiber contents had a significant effect on the UPPT, especially after loading, with more substantial discrepancies between the DMM and IMM as fiber contents increased. Additionally, matrices with vertical notches exhibited relatively stable UPPT changes, regardless of the measurement technique used. The differences in UPPT values between the two methods are primarily attributed to wave dispersion, longer propagation paths, and greater energy loss in the IMM, all contributing to an increase in propagation time.
- The presence of vertical notches significantly influences UPPT in matrices, with an increase observed under both pre-loading and post-loading conditions. Before loading, UPPT in SF10N1 rose by 17.3% (IMM) and 18.3% (DMM) compared to SF10N0. After loading, the increases were 30% for IMM and 2.1% for DMM. As cracks widen and deepen under bending stress, the pulse travels a longer distance, leading to stronger wave reflections and delayed arrival times. Steel fibers, by bridging cracks, help prevent sudden failure, facilitating measurable pulse propagation even after bending loads are applied.
- As bending stress increases and cracks begin to form and propagate, the UPPT in matrices becomes unstable, exhibiting fluctuations with each transition. Moreover, once the stress exceeds 100%, excessive crack expansion leads to signal discontinuity, resulting in a rapid increase in UPPT. This increase in UPPT is primarily caused by the dispersion of pulse energy, as deeper cracks obstruct the effective transmission of the pulse

signal, hindering its progression through the matrices.

- The mechanical properties of HPFRC are significantly influenced by the steel fiber content. The compressive strength of HPFRC rises as the fiber content increases up to 1.0%, but declines at 2.0% for challenges such as fiber agglomeration and reduced workability. The compressive strengths of SF00N0, SF05N0, and SF10N0 were 63.95 MPa, 92.88 MPa, and 101.31 MPa, respectively, while SF20N0 exhibited a lower value of 86.06 MPa. The flexural strength of HPFRC also improves with higher fiber percentages, particularly at 0.5%, 1.0%, and 2.0%. In particular, smaller specimens exhibited a more significant increase in flexural strength, likely due to more consistent fiber dispersion.

This study provided the main factors influencing UPPT in HPFRC, offering valuable insights for engineering practice. Key findings included the positive effect of steel fibers on post-cracking pulse transmission, as well as the impact of specimen size, testing methods, and notches on UPPT values. These results guide decisions on fiber dosage, specimen design, and testing procedures for the reliable use of HPFRC in structural applications.

6. ACKNOWLEDGMENTS

This research was supported by the Basic Research Program funded by the Education and Training Ministry (Project B2023-MDA-06). The opinions expressed in this paper are those of the authors and do not necessarily reflect the views of the sponsors.

7. REFERENCES

[1] Li J., Wu Z., Sh, C., Yuan Q., and Zhang Z., Durability of ultra-high performance concrete – A review. Construction and Building Materials, Vol. 255, 2020, pp. 119296, doi: 10.1016/j.conbuildmat.2020.119296

[2] Saloma and Sulthan.F., Influence of Hooked-End Steel Fibers on Flexural Behavior of Steel Fiber Reinforced Self-Compacting Concrete (Sfrscc). International Journal of GEOMATE, Vol. 23, Issue 95, 2022, pp. 127–135, doi: 10.21660/2022.95.3310.

[3] Yousefieh N., Joshaghani A., Hajibandeh E., and Shekarchi M., Influence of fibers on drying shrinkage in restrained concrete. Construction and Building Materials, Vol. 148, 2017, pp. 833–845. 10.1016/j.conbuildmat.2017.05.093.

[4] Diamond S. and Huang J., The ITZ in concrete - A different view based on image analysis and SEM observations. Cement and Concrete Composites, Vol. 23, No. 2–3, 2001, pp. 179–188. doi: 10.1016/S0958-9465(00)00065-2.

[5] Brown M., Wright D., M'Saoubi R., McGourlay J., Wallis M., Mantle A., Crawforth P., and Ghadbeigi H., Destructive and non-destructive testing methods for characterization and detection of machining-induced white layer: A review paper. CIRP Journal of Manufacturing Science and Technology, Vol. 23, 2018, pp. 39–53, doi: 10.1016/j.cirpj.2018.10.001.

[6] Nainggolan C.R., Wijatmiko I., Suseno H., and Firdausy A.I., Study of Distance and Number of Rebars on Velocity Measurement Using Non-Destructive Test. International Journal of GEOMATE, Vol. 22, Issue 94, 2022, pp. 121–127, doi: 10.21660/2022.94.1747.

[7] Saint-Pierre F., Philibert A., Giroux B., and Rivard P., Concrete Quality Designation based on Ultrasonic Pulse Velocity. Construction and Building Materials, Vol. 125, 2016, pp. 1022–1027, doi: 10.1016/j.conbuildmat.2016.08.158.

[8] Tan Y., Yu H., Mi R., and Zhang Y., Compressive strength evaluation of coral aggregate seawater concrete (CAC) by non-destructive techniques. Engineering Structures, Vol. 176, 2018, pp. 293–302, doi: 10.1016/j.engstruct.2018.08.104.

[9] AL-Ridha A.S.D., Atshan A.F., Abbood A.A., and Dheyab L.S., Effect of Steel Fiber on Ultrasonic Pulse Velocity and Mechanical Properties of Self-Compact Concrete. International Journal of Innovative Research in Science, Engineering and Technology, Vol. 6, No. 8, 2017, pp. 022017, doi: DOI:10.15680/IJIRSET.2016.0608223.

[10] Parihar H.S., Shanker R., and Singh V., Effect of variation of steel reinforcement on ultrasonic pulse velocity prediction in concrete beam. Materials Today: Proceedings, Vol. 65, 2022, pp. 1486–1490, https://doi.org/10.1016/j.matpr.2022.04.468.

[11] Petro J.T. and Kim J., Detection of delamination in concrete using ultrasonic pulse velocity test. Construction and Building Materials, Vol. 26, No. 1, 2012, pp. 574–582, doi: 10.1016/j.conbuildmat.2011.06.060.

[12] Malhotra V.M. and Carino N.J., Handbook on Nondestructive Testing of Concrete. CRC Press, 2004, pp.1–200.

[13] Le H.V., Pham T.N., Dang V.P., Dao P.L., Nguyen D.L., Tran N.T., and Kim D.J., Damage sensing characteristics of smart ultra-high-performance concrete containing electrically conductive fiber and particle fillers under high compressive stress. Sensors and Actuators: A. Physical, Vol. 383, 2025, pp.116-242, doi: 10.1016/j.sna.2025.116242.

[14] Wu Z., Shi C., He W., and Wu L., Effects of steel fiber content and shape on mechanical properties of ultra high performance concrete. Construction and Building Materials, Vol. 103, 2016, pp. 8–14, doi: 10.1016/j.conbuildmat.2015.11.028.

[15] Bazant Z.P., Size effect on structural strength: a

review. Archive of Applied Mechanics, Vol. 69, 1999, pp. 703–725, https://doi.org/10.1007/s004190050252.

[16] Ju M., Park K., and Oh H., Estimation of Compressive Strength of High Strength Concrete Using Non-Destructive Technique and Concrete Core Strength. Applied Sciences, Vol. 7, No. 12, 2017, pp. 1249, doi: doi:10.3390/app7121249.

[17] Yu T., Chaix J.F., Audibert L., Komatitsch D., Garnier V., and Hénault J.M., Simulations of ultrasonic wave propagation in concrete based on a two-dimensional numerical model validated analytically and experimentally. Ultrasonics, Vol. 92, 2019, pp. 21–34, doi: 10.1016/j.ultras.2018.07.018.

[18] Al-Ridha A.S.D., Ibrahim A.K., Al-Taweel H.M., and Dheyab L.S., Effect of Steel Fiber on Ultrasonic Pulse Velocity and Mechanical Properties of Self-Compact Light Weight Concrete. IOP Conference Series: Materials Science and Engineering, Vol. 518, No. 2, 2019, pp. 130–139, doi: 10.1088/1757-899X/518/2/022017.

[19] Shankar S., and Joshi H.R., Comparison of Concrete Properties determined by Destructive and Non-Destructive Tests. Journal of the Institute of Engineering, Vol. 10, No. 1, 2014, pp. 130–139, doi: 10.3126/jie.v10i1.10889.

[20] Oh S.C., Comparison of ultrasonic velocities between direct and indirect methods on 30 mm × 30 mm spruce lumber. Journal of Korean Wood Science and Technology, Vol. 48, No. 4, 2020, pp. 562–568, doi: 10.5658/WOOD.2020.48.4.562.

[21] Filonidov A. M., Relation between ultrasound propagation velocity and path length in solid concrete. Hydrotechnical Construction, No. 2, pp. 32–36, 1970, doi: https://doi.org/10.1007/BF02377235.

[22] Lin J., Tian B., Liang Z., Hu E., Liu Z., Wang K., Sang T., Impact of Water–Cement Ratio on Concrete Mechanical Performance: Insights into Energy Evolution and Ultrasonic Wave Velocity. Materials, Vol.17, 2024, pp. 365 https://doi.org/10.3390/ma17153651.

[23] Benaicha M., Jalbaud O., Hafidi A., and Burtschell Y., Correlation between the mechanical behavior and the ultrasonic velocity of fiber-reinforced concrete. Construction and Building Materials, Vol. 101, 2015, pp. 702–709, doi: 10.1016/j.conbuildmat.2015.10.047.

[24] Pinto R.C., Medeiros A., Padaratz I., and Andrade P.B, Use of Ultrasound to Estimate Depth of Surface Opening Cracks in Concrete Structures. e-Journal of Nondestructive Testing, 2010. https://www.ndt.net/?id=9954

[25] Gao Y., and Sun H., Influence of initial defects on crack propagation of concrete under uniaxial compression. Construction and Building Materials, Vol. 277, 2021, pp. 122-361, doi: 10.1016/j.conbuildmat.2021.122361.

[26] Series C., Directivity of guided ultrasonic wave scattering at notches and cracks. Journal of Physics: Conference Series, Vol. 269, 2011, pp. 012018, doi: 10.1088/1742-6596/269/1/012018.

[27] Ham S., Song H., Oelze M.L., and Popovics J.S., A contactless ultrasonic surface wave approach to characterize distributed cracking damage in concrete. Ultrasonics, Vol. 75, 2017, pp. 46–57, doi: 10.1016/j.ultras.2016.11.003.